

SUPPRESSION OF HOMs IN A MULTICELL SUPERCONDUCTING CAVITY FOR CORNELL'S ERL*

Valery Shemelin[#], Cornell Laboratory for Accelerator-based Sciences and Education (CLASSE),
Ithaca, NY, U.S.A.

Abstract

Minimization of power of higher order modes (HOMs) in a multicell cavity was done using derivatives of the parameter defining losses with respect to geometric parameters of the cavity cells. For the Cornell Energy Recovery Linac most dangerous are dipole modes causing beam break-up (BBU). As a start point of optimization the shape with minimal losses at the fundamental mode was taken. Further changing the shape for better propagation of HOMs was done with degradation of the fundamental mode loss parameter (GR/Q) within 1 % while decrease of the BBU parameter was nearly 3 orders of magnitude. The BBU threshold current tends to be inversely proportional to this parameter.

INTRODUCTION

Optimization of a SC cavity for minimal losses of the fundamental mode power is necessary because these losses define the major part of total power needed for cryogenics in the CW operation. On the other hand, the current in the accelerator is limited by HOMs excited in the cavities by the electron bunches, and to minimize this detrimental effect one should change this initially found "best" shape.

We suppose to resolve this contradiction in the following way. (1) To find the best shape of the inner and end cells of the cavity from the view point of minimal losses. (2) To change the shape of the end cells, even end half-cells only, to improve coupling between the cavity and the beam pipes keeping the increase of fundamental losses in the end cells at some limited level. The losses will increase in the end cells only, so the total relative increase will be smaller for a multicell cavity. (3) If necessary, change the shape of the inner cells, keeping in mind their bigger contribution into total losses.

The problem of the search for the shape with minimal losses was studied in details earlier [1] and there it was also stated that wide deviations of some geometric parameters do not spoil much the loss parameters of the cells if only these deviations are compensated by changing some other geometric parameters. As these changeable geometric parameters, the half-axes of elliptic arcs forming the cell contour were used. This property of compensation was supposed as the future resource for HOMs tuning.

LIMITATIONS FOR THE PEAK FIELD AND GEOMETRIC PARAMETERS

We should impose some limitation on the cell shape due to computational, technological and other conditions. First of all, we will discuss the elliptic shape of the cells, Fig. 1. This means that the half-cell consists of two elliptic arcs connected with a conjugated straight segment. Four half-axis, A , B , a , and b , of the cells can be treated as independent variables whereas the equatorial radius R_{eq} , is used for tuning the cell to the working frequency f . In this paper we will use dimensions corresponding to $f = 1300$ MHz chosen for the Cornell ERL. We shall deal with the π -mode of the standing wave in the cavity, so the length of the inner half-cell will be $L = \lambda/4$, quarter of the wave length.

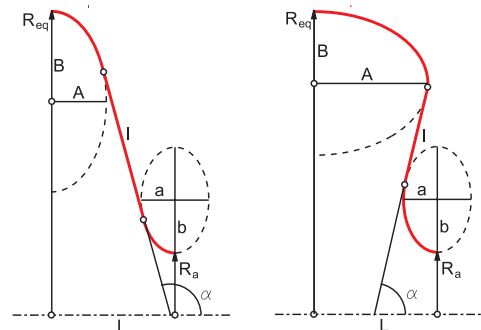


Figure 1: Geometry of the inner cell: non-reentrant (left) and reentrant (right) shapes.

We should choose limitations for the cell wall slope angle. In spite of better loss properties of the reentrant shape [2], Fig. 1, this shape is still in a stage of detailed investigations in our lab and elsewhere and now we will discuss more traditional, non-reentrant shape. Nevertheless, the angle α of the wall slope should be given, and we will take $\alpha = 95^\circ$, trying to come closer to the angles $\alpha < 90^\circ$ but still to be on the traditional side of this barrier.

The next limitation is connected with normalized peak surface field E_{pk}/E_{acc} , where E_{pk} is maximal electric field on the surface and E_{acc} is the acceleration V_{acc} in the cell in Volts divided by $\lambda/2$. This definition, $E_{acc} = V_{acc}/(\lambda/2)$ instead of $E_{acc} = V_{acc}/L_{cell}$, where L_{cell} is the geometric length of the cell, should be kept for the end cell also because its active length is not defined: field is penetrating into the beam pipe and actually we are interested in voltage on the cell, the length of the end cell is not very important. Increasing the value

* Work has been supported by NSF Award PHY-0131508, Empire State Development Corporation, and Cornell University.

[#] vs65@cornell.edu

of E_{pk}/E_{acc} , one can decrease maximal normalized magnetic field H_{pk}/E_{acc} and losses in the cell. Minimization of H_{pk}/E_{acc} also gives a possibility to achieve the maximal accelerating rate E_{acc} in the cavity because the magnetic field is a hard limit for the SC niobium and the electric field is a soft limit [3]. However, too high E_{pk}/E_{acc} will lead to the field emission, and we should be limited by reasonable value of it. In the case of Cornell ERL we took a conservative value $E_{pk}/E_{acc} = 2$.

The basic geometric parameter which we will take as a given one, is the iris aperture R_a . Smaller values of R_a decrease losses of the fundamental mode but strongly increase problems with HOMs. We will rely upon TESLA experience and take for the inner cells $R_a = 35$ mm.

The higher order modes should have a possibility to propagate to the load through the beam pipe. So, the radius of the beam pipe should be above the cut-off value of the lowest HOMs. In the TESLA cavities [4] the beam pipe radius is $R_{bp} = 39$ mm. This corresponds to the cut-off frequency of the dipole mode equal to $f_c = 2253$ MHz. For the geometry chosen for the ERL cavity, only modes of the 3rd dipole band and higher can propagate through this beam pipe. The lowest modes of the first band have their frequency near 1600 MHz but can be tuned for our geometry to about 1700 MHz. To guarantee a possibility of their extraction, we choose the beam pipe radius $R_{bp} = 55$ mm with a cut-off frequency of 1597 MHz and decided to make the beam pipes on different sides of the cavity with different inner radii: $R_{bpa} = 39$ and $R_{bpb} = 55$ mm.

We will keep the smaller radius from one side of the cavity because in the case of a broad beam pipe we need to place the HOM load further from the cavity to prevent degradation of quality factor of the fundamental (accelerating) mode. We are forced to use a broad pipe but can use it from one only side of the cavity to make the whole cavity shorter. The solution with a broad pipe was not used in the TESLA cavity, possibly because the need to suppress HOMs was not as essential as it is in the case of ERL.

Trying not to loose accelerating properties of the end cell with a broad pipe, we will use an iris between the cavity and the broad pipe. So, the end cells will be of two kinds, Fig. 2, let us call them “end cells of type *a*, and type *b*”.

Radius of curvature $R_{ce} = a_e^2/b_e$ of the transition from the half cell to the beam pipe (type *a*) or to the other half of the iris (type *b*) cannot be too small because of difficulties of stamping, in our case we will take it not smaller than 6 mm. The same is true for the end half-iris (type *b*), in this case we will keep also $R_{ct} = a_t^2/b_t \geq 6$

mm. At the same time, in optimization of the fundamental mode, it appeared that the sum $R_{ce} + R_{ct}$ for the type *b* end cell tends to become infinitely big that is the same as a choice of a narrower pipe. To exclude this case let us limit this value by 15 mm as we did in [1]. Further, if it will help in propagation of HOMs, we can increase the value of this limitation. For simplification values of a_t and b_t are chosen to be 6 mm.

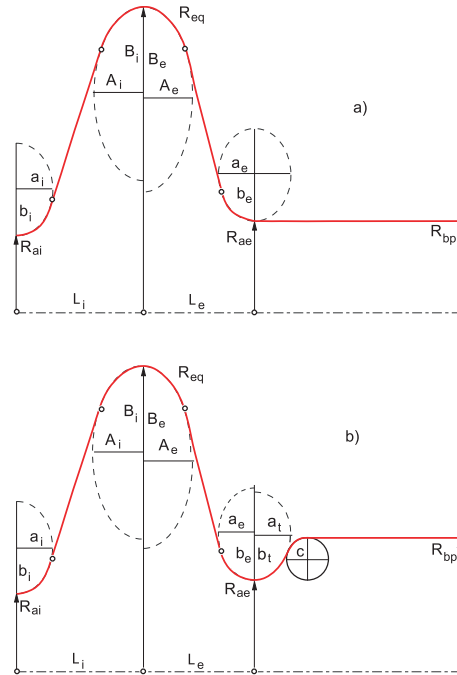


Figure 2: Two possible end cells of a multicell cavity: type *a* - with a simple transition to the beam pipe (a), and type *b* - with an iris in a broader beam pipe.

Radius c of the transition between the end cell iris and the beam-pipe should be big enough, about $c = 2 \cdot (R_{bp} - R_{ae})$, here R_{ae} is the aperture of the end iris. This is necessary to exclude a possibility of multipacting in the minimum of RF electric field which can appear otherwise in this transition [5].

MODEL OF HOM LOAD FOR SIMULATION

If we optimize the end cells for better propagation of HOMs which frequencies are over the cut-off, we should have a non-reflecting load at some distance from the end cell at each side of the cavity. For the free space such a load is known: having the impedance of material $Z = \sqrt{\mu\mu_0/\epsilon\epsilon_0}$ of the same value as the impedance of free space $Z_0 = \sqrt{\mu_0/\epsilon_0}$, we should have relative permeability and permittivity of the material equal and having non-zero imaginary parts, for example, $\mu = \epsilon = 1 - i$, we will have full absorption if the thickness of the absorber is big enough. Unfortunately, in the waveguide, the impedance has dispersion, and such a perfect absorber cannot be realized neither in simulation

all the more in practice. The impedance has different dependences on frequency for TE waves, $Z_{TE} = Z_0 \mu / \sqrt{\epsilon \mu - (\lambda/\lambda_c)^2}$, and for TM waves, $Z_{TM} = (Z_0/\epsilon) \cdot \sqrt{\epsilon \mu - (\lambda/\lambda_c)^2}$, where λ is the wave length in the free space and λ_c is the cut-off wave length of an empty waveguide.

The reflection coefficient from the interface between an empty and a filled waveguide can be found for the TE-wave as

$$\Gamma = \frac{\sqrt{1 - (\kappa/\mu)^2} - \sqrt{1 - \kappa^2}}{\sqrt{1 - (\kappa/\mu)^2} + \sqrt{1 - \kappa^2}},$$

where $\kappa = \lambda_0/\lambda_c$; for the TM-waves μ in the equation for Γ should be changed by ϵ . If we take the loss tangent equal to 1, we can see, Fig. 3, that Γ very weakly depends on absolute value of ϵ and μ . For simplicity of the mesh in the simulation of the lossy stuff, we will take $\mu = \epsilon = 1 - i$.

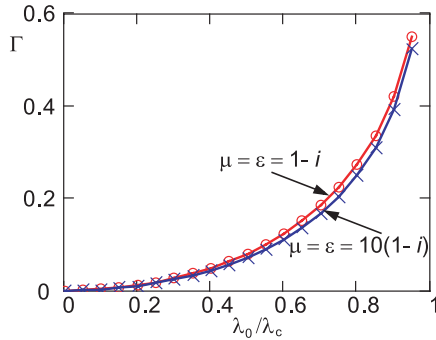


Figure 3: Coefficient of reflection from the lossy material in the waveguide.

One can see that for the 10 % shorter wave length than the cut-off wave length, the reflection is equal to $\Gamma = 0.5$ or only 25 % in power. Absorption of three quarters of power propagating into the pipe will secure very low Q of the mode if the coupling with the pipe is big enough.

The ideal absorption can be found if we calculate the external quality factor Q_{ext} of the cavity. Calculation of the Q_{ext} is analyzed in [6]. For the case of the round waveguide with a TE_{11} wave we can find $Q_{ext} = Q_E + Q_H$, where Q_E and Q_H are defined when different boundary conditions are imposed at the end of the waveguide:

$$Q_E = \frac{2U\Lambda}{\epsilon_0 a^2 \lambda^2 E_m^2 (1 - 1/v_{11}^2) \cdot J_1^2(v'_{11})},$$

$$Q_H = \frac{2U}{\mu_0 a^2 \Lambda H_e^2 (1 - 1/v_{11}^2) \cdot J_1^2(v'_{11})},$$

where U is total energy in the cavity, Λ and λ are wavelengths in the waveguide and in the free space, respectively, a is the radius of the waveguide, E_m is

maximal electric field on the magnetic wall at the butt of the waveguide, H_e is maximal magnetic field on the electric wall at the butt of the waveguide, $J_1(v'_{11})$ is the Bessel function of the first kind at the point of the first root of the derivative $J_1'(x)$.

In the model the load is a disc at the butt of the pipe filled with the lossy material, Fig. 4. A half-cavity with a magnetic wall at the left boundary was used for this simulation. The structure of the electric field of a mode with a low coupling with the load is also presented in the picture.

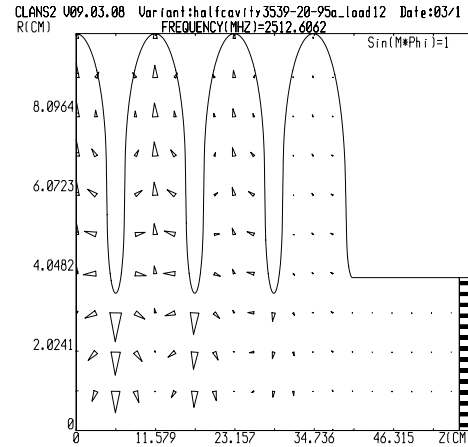


Figure 4: A half-cavity with a disc-shape load at the end of the beam-pipe for the data presented at Figure 5 and a dipole mode with high Q_{ext} .

Comparison of results with the lossy load in the beam pipe of radius $R_{bp} = 39$ mm having $\mu = \epsilon = 1 - i$ and results with calculated Q_{ext} according to above mentioned procedure is shown in Fig. 5. The relevant values of the BBU parameter p are also presented. Its change with the transition from the modeled load to the ideal one is practically the same as of Q because R/Q weakly depends on Q . The BBU parameter on this figure is big because this calculation is done before its optimization. Here the modes of the 3rd dipole band were examined.

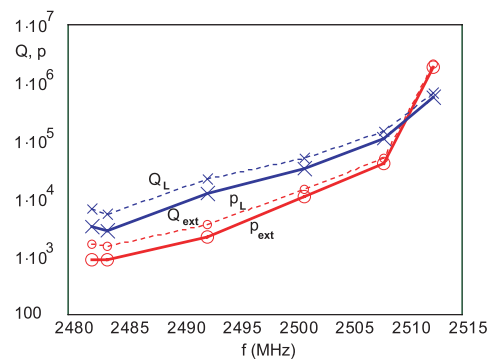


Figure 5: Q_{ext} and BBU parameter p [Ohm/cm²/GHz] for the cavity optimized for minimum losses, before HOM optimization.

One can see that the ideal Q_{ext} is about 2 times lower than the loaded Q_L at the lowest frequency of this band, and only 20 % lower at the highest frequency. Let us remind that the cut-off frequency is $f_c = 2253$ MHz, less than 10 % lower than the lowest frequency of this band. It is clear that for highest bands of HOMs the load with $\mu = \varepsilon = 1 - i$ can be treated as a good one.

For the 1st dipole band, we have a smaller margin than for the 3rd one, approximately 1700 MHz versus 1600 MHz, *i. e.* about 6 %. However, as we will see later, there are no problem with coupling of these modes with the pipe, and, moreover, the ideal Q_{ext} (and, hence, p) is always less than in the model. Of course, we cannot find the best solution with the non-ideal load but we still can find a geometry which has a significant coupling with the load.

Final optimization will be done with the model of a real HOM load which (1) is far from the ideal in the shape, it cannot fill the whole pipe; and (2) is far from ideal in the electromagnetic properties of the lossy material. However, we will try to separate again our task: first we separated optimization of the fundamental mode and HOMs, now we are trying to separate optimization of the HOMs extraction and their absorption by the load.

USAGE OF DERIVATIVES $\partial p/\partial q$

We can find derivatives $\partial p/\partial q$ of the BBU parameter with respect to any size of the end half-cells' half-axes: so that $q = A_a, B_a, \dots, a_b$, or b_b . We can do this for any HOM dipole mode. Having the matrix of $\partial p/\partial q$, we can minimize the maximal value of p for a given frequency range. We will limit the task by 8 most dangerous modes, *i. e.* the modes with biggest p . For the transition radius $R_{ae} = R_{aea} = 39$ mm for the type *a* end half-cell and $R_{ae} = R_{aeb} = 39$ mm for the type *b* end half-cell (Fig. 2), such a matrix is presented in Fig. 6, for frequencies shown in the upper line and values of p shown in the lower line. Values of q are shown in the column on right.

f:	1739	1867	1883	2467	2511	2513	3073	3400	q
$dp/dq =$	-87	-19	21	0	-5024	7001	1427	-248	A_a
	30	9	-5	0	2180	-1957	-508	147	B_a
	0	-1	-2	0	-107	-166	-35	105	a_a
	4	-3	-6	0	119	-144	-65	18	b_a
	221	-102	-145	261	-28	-16	279	-53	A_b
	-95	27	41	69	12	6	-92	26	B_b
	86	37	63	-43	0	0	-26	-8	a_b
	-20	-5	-4	-5	0	0	5	-2	b_b
p:	2270	1209	2158	1918	2261	2259	2145	2259	

Figure 6: Matrix of derivatives $\partial p/\partial q$ and associated frequencies, p 's, and q 's.

The values of p were decreased nearly 3 orders of magnitude from the initial geometry when all the cells had minimal fundamental losses, Fig. 7. A very high BBU threshold [7], about 10 A, corresponds to this new geometry. The value of GR/Q , defining fundamental losses in the cavity decreased in this optimization only by 4.6 % for the type *a* cell and by 1.1 % for the type *b* (broader) cell. Since the losses in the inner cell did not change, the total drop of GR/Q , *i.e.* increase of losses, in a 7-cell cavity will be 0.8 % only. Unfortunately small deviations of the shape lead to dramatic increase of p [8] and further decrease of the maximal p is desirable. From a general point of view, a decrease of the BBU parameter p should lead to a decrease of its derivatives $\partial p/\partial q$ because the value of p is limited from below. This should lead to a weaker sensitivity to disturbances of dimensions. However, another possibility to decrease this sensitivity exists: broadening of the HOMs band widths [8].

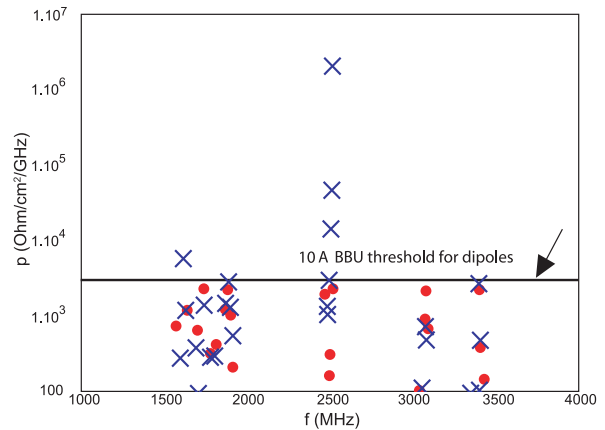


Figure 7: BBU parameter p vs frequency for the cavity with minimal fundamental losses before and after optimization for minimal p .

Further decrease of p is limited by behavior of derivatives for two modes: 2511 and 2513 MHz, see Fig. 6. The biggest derivatives correspond to half-axes A_a and B_a but they have different signs. Values of p for these two modes are nearly equal: 2261 and 2259. So, further improvement of p can be done by changing other half-axes, but it will be insignificant.

From Fig. 6, one can see that lowest modes are more sensitive to the change of the type *b* end cell (left lower quarter of the matrix) whereas the higher modes depend strongly on the type *a* cell, with the smaller pipe (right-hand upper quarter). This means that the lowest HOMs are directed to the broader pipe and the higher modes propagate to the smaller pipe though they could be tuned for propagation into the broader pipe as well. The example pictures of electric field of these modes confirm the aforesaid, Fig. 8.

An attempt to redirect the lowest mode of the two with highest $\partial p/\partial q$ ($f = 2511$ and 2513) was made. This separation was successful, Fig. 9, frequencies of the modes somewhat changed: to 2514 and 2517 MHz.

Unfortunately, after this procedure several other modes substantially increased their BBU parameter and this attempt was left aside.

Further improvement of the geometry can be done using the same procedure of decreasing the BBU

parameter- for the inner cells. This tuning for lower p can be closely related to the broadening of the band width of the HOMs.

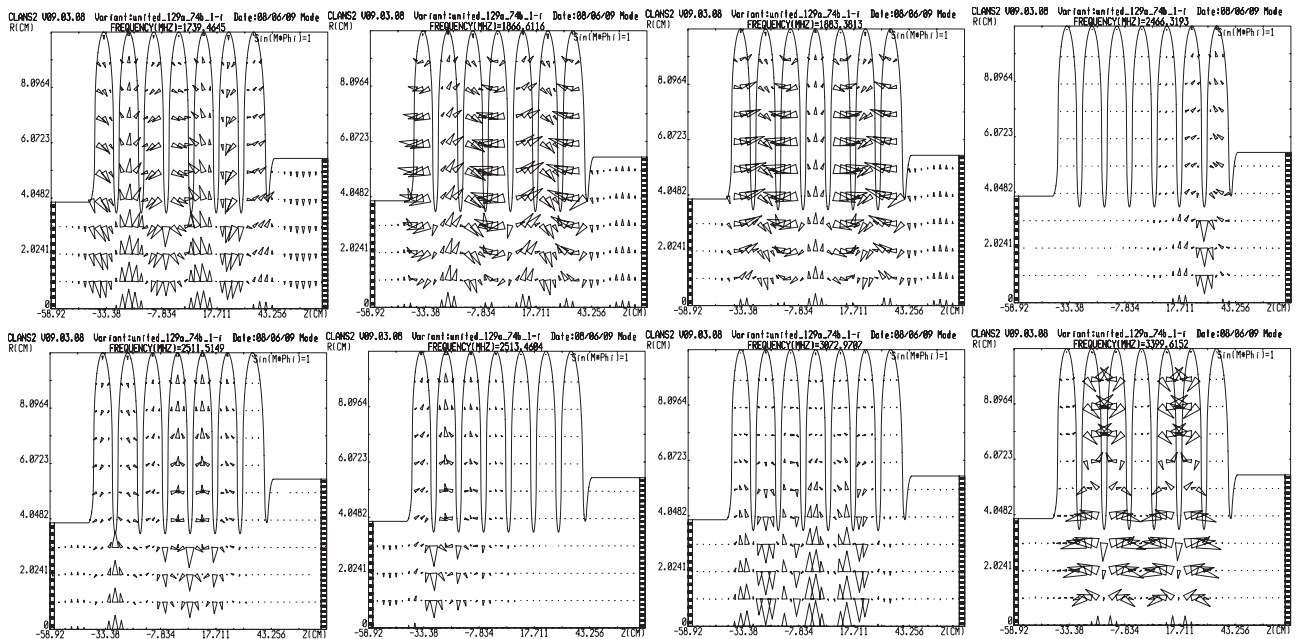


Figure 8: Electric field of eight modes with biggest p .

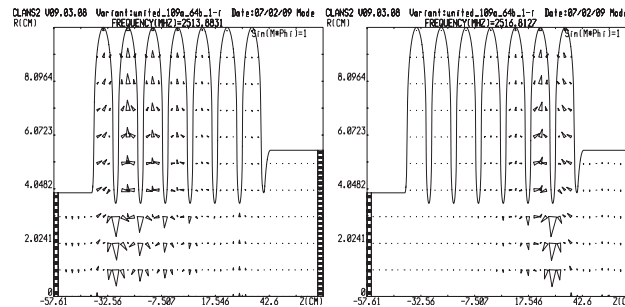


Figure 9: Redirection of modes with maximal $\partial p/\partial q$ into different pipes.

CONCLUSIONS

A possibility to control tuning of the HOMs propagation into the beam pipes was demonstrated. Usage of derivatives of the BBU parameter with respect to cell dimensions is a powerful method of suppression of the HOMs. Minimization of the BBU parameter of dipole HOMs was done changing the shapes of the end half-cells of the cavity with increase of power losses of the fundamental mode by 0.8 %. Decrease of the BBU parameter was nearly 3 orders of magnitude compared to the original shape tuned for minimal losses. The BBU threshold current was increased the same value, up to 10 A.

REFERENCES

[1] V. Shemelin, "Optimal choice of cells geometry for a multicell superconducting cavity", Phys. Rev. Spec. Topics – Acc. and Beams, in print.

[2] V. Shemelin, "Low loss and high gradient SC cavities with different wall slope angles", Proc. PAC 2007, p. 2352-2354, Albuquerque, New Mexico, USA, June 25 – 29, 2007.

[3] K. Saito, Proc. SRF 2001, p. 583-587, Tsukuba, Japan, Sep. 6 – 11, 2001.

[4] B. Aune et al., "Superconducting TESLA cavities," Phys. Rev. Spec. Topics – Acc. and Beams **3**, 092001 (2000).

[5] Sergey Belomestnykh, Valery Shemelin, Nucl. Instr. Meth. Phys. Res. A **595**, 293-298 (2008).

[6] V. Shemelin, S. Belomestnykh, Cornell LEPP Report SRF 020620-03, 2002.

[7] I. Bazarov, G. Hoffstaetter, "Multi-pass beam-breakup: theory and calculation", EPAC 2004, Lucerne (2004).

[8] M. Liepe, N. Valles, "Seven-cell cavity optimization for Cornell's Energy Recovery Linac", this Workshop.